Kinetochore Microtubule Dynamics and the Metaphase–Anaphase Transition

Ye Zhai, Paul J. Kronebusch, and Gary G. Borisy

Laboratory of Molecular Biology, University of Wisconsin-Madison, Madison, Wisconsin 53706

Abstract. We have quantitatively studied the dynamic behavior of kinetochore fiber microtubules (kMTs); both turnover and poleward transport (flux) in metaphase and anaphase mammalian cells by fluorescence photoactivation. Tubulin derivatized with photoactivatable fluorescein was microinjected into prometaphase LLC-PK and PtK_1 cells and allowed to incorporate to steady-state. A fluorescent bar was generated across the MTs in a half-spindle of the mitotic cells using laser irradiation and the kinetics of fluorescence redistribution were determined in terms of a double exponential decay process. The movement of the activated zone was also measured along with chromosome movement and spindle elongation. To investigate the possible regulation of MT transport at the metaphase-anaphase transition, we performed double photoactivation analyses on the same spindles as the cell advanced from metaphase to anaphase. We determined values for the turnover of kMTs ($t_{1/2}$ = 7.1 ± 2.4 min at 30°C) and demonstrated that the turnover of kMTs in metaphase is approximately an order of magnitude slower than that for non-kMTs. In anaphase, kMTs become dramatically more stable as evidenced by a fivefold increase in the fluorescence redistribution half-time ($t_{1/2}$ = 37.5 ± 8.5 min at 30°C). Our results also indicate that MT transport slows abruptly at anaphase onset to one-half the metaphase value. In early anaphase, MT depolymerization at the kinetochore accounted, on average, for 84% of the rate of chromosome movement toward the pole whereas the relative contribution of MT transport and depolymerization at the pole contributed 16%. These properties reflect a dramatic shift in the dynamic behavior of kMTs at the metaphase-anaphase transition.

A release–capture model is presented in which the stability of kMTs is increased at the onset of anaphase through a reduction in the probability of MT release from the kinetochore. The reduction in MT transport at the metaphase-anaphase transition suggests that motor activity and/or subunit dynamics at the centrosome are subject to modulation at this key cell cycle point.

UNDERSTANDING the behavior of kinetochore microtubules is important because the attachment of chromosomes to the spindle and chromosomal motions throughout mitosis are clearly tightly coupled to the nature of the interaction between the components of the kinetochore and the microtubules (MTs)[1] bound to them (for reviews see Mitchison, 1988; McIntosh and Hering, 1991). The attachment must be strong enough to support the frictional drag on the chromosome during the movements of congression and anaphase, yet labile enough to permit the breakage of incorrect attachments and the correction of malorientations during prometaphase (Nicklas, 1988). Over the last few years it has become apparent that spindle MTs can exhibit two kinds of dynamic behavior; turnover through the property of dynamic instability (Mitchison and Kirschner, 1984) and poleward transport sometimes referred to as flux (Mitchison, 1989).

Fluorescence photobleaching recovery experiments have shown that MTs turn over rapidly in the mitotic spindle (Salmon et al., 1984*b*; Saxton et al., 1984; Wadsworth and Salmon, 1986; Hamaguchi et al., 1987; Cassimeris et al., 1988; Gorbsky et al., 1990; Hush et al., 1994). The mechanism by which this turnover takes place is characterized by a process termed dynamic instability (Mitchison and Kirschner, 1984). Although there is general agreement that most MTs turn over more rapidly in mitosis than in interphase (for review see Gelfand and Bershadsky, 1991), the mitotic spindle is a mixed population of kinetochore fiber microtubules (kMTs) and non-kMTs and their dynamics are likely to differ. In mammalian cells cultured under normal conditions, kMTs comprise only a minority population, estimated from electron microscopy as approximately 20 to 25% of all spindle MTs at 37°C (Brinkley and Cartwright, 1971; McIntosh et al., 1975; Rieder, 1981*a*;

Address correspondence to G. G. Borisy, University of Wisconsin-Madison Laboratory of Molecular Biology, R. M. Bock Laboratories, 1525 Linden Dr., Madison, WI 53706-1596. Tel.: (608) 262-4581; Fax: (608) 262-4570.

1. *Abbreviations used in this paper*: MT, microtubule; kMTs, kinetochore fiber microtubules; MAP, MT-associated protein; non-kMTs, non-kinetochore microtubules.

Wise et al., 1991). Our recent study of MT polymer levels in LLC-PK cells using a quantitative fluorescence ratio method, gave a value of 57% for the proportion of tubulin in polymer in the metaphase spindle at 37°C (Zhai and Borisy, 1994), meaning that 43% of the cellular tubulin was in the soluble pool. Multiplying the polymer proportion of 57% by the proportion of kMTs of 20–25% gives a value for the kMTs of 10–15% of total cellular tubulin. Thus, the kMTs represent only a small proportion of the total fluorescence signal and the fluorescence redistribution after photobleaching presumably was dominated by the kinetic behavior of soluble tubulin and non-kMTs. A minor component found not to exchange on the time scale of the analysis was commonly observed and could have represented kMTs (Wadsworth and Salmon, 1986; Cassimeris et al., 1988, 1990; Gorbsky and Borisy, 1989). In addition, as judged by susceptibility to depolymerization induced by cold (Brinkley and Cartwright, 1971, 1975; Rieder, 1981*a*,*b*; Wise et al., 1991), pressure (Salmon et al., 1976), or tubulin-binding drugs (Salmon et al., 1984*a*), kMTs were clearly indicated to be more stable than non-kMTs. One quantitative study, using nocodazole-induced depolymerization and correlative electron microscopy, gave a kMT lifetime of 7.5 min at 23°C (Cassimeris et al., 1990). However, since all of these studies involved departures from the steady-state, arguments could be made that the differential stability of kMTs was induced by the applied treatment and did not reflect a true stability in vivo. In a study using immunogold electron microscopy, metaphase cells were injected with biotinylated tubulin and then fixed 5–14 min later, after the initiation of anaphase (Mitchison et al., 1986). Approximately half of the kMTs did not show biotin label indicating that they had failed to incorporate tubulin during the period after injection. Although these studies suggested the existence of a class of spindle MTs that turned over slowly, a quantitative evaluation of MT turnover times from electron microscopic data was not feasible.

An additional issue is whether kMT dynamics change at the metaphase-anaphase transition. Although several groups have analyzed spindle MT dynamics in prometaphase and metaphase, little data is available concerning anaphase. Gorbsky and Borisy (1989) compared metaphase and anaphase MT dynamics by photobleaching living cells but then lysing them in a cold, Calcium-containing buffer to selectively depolymerize non-kMTS. In this way, they obviated the contributions of the soluble tubulin pool and the more labile non-kMTs, and were able to show that kMTs in anaphase, although in the process of shortening, were otherwise apparently stable, that is, showed no measurable fluorescence recovery. This study and previous qualitative studies which reported persistent photobleached marks on anaphase MTs in an analysis of sites of MT depolymerization (Gorbsky et al., 1987, 1988) pointed to the possibility of a shift in MT dynamics at the metaphase–anaphase transition.

In addition to dynamic instability, there is a second type of dynamics. Previous photobleaching and photoactivation experiments have detected a slow poleward transport of tubulin subunits occurring at metaphase in LLC-PK and PtK cells (Gorbsky and Borisy, 1989; Mitchison, 1989) and during both metaphase and anaphase in newt lung cells (Mitchison and Salmon, 1992), signifying that the centrosome as well as the kinetochore attachments of the kMTs are dynamic. Photoactivation studies demonstrated long lived kMTs and a poleward flux of tubulin subunits, but as the focus of these studies was on flux and the imaging technology used (SIT video camera) had insufficient dynamic range for quantitative analysis, the turnover of the kMTs per se was not examined in detail.

In the experiments reported in this paper, we have used the photoactivation technique to make quantitative measurements of kMT turnover and transport in metaphase and anaphase with emphasis on the issue of whether this process is regulated at the metaphase–anaphase transition. Turnover can be viewed as a measure of behavior of the kMT plus ends and poleward transport as a measure of minus end activity. We find that both the kMT turnover and poleward transport behavior of kMTs changes significantly at the metaphase–anaphase transition. The differential stability of kMTs with respect to non-kMTs is interpreted in terms of a release–capture model, and the shift in dynamics at the metaphase–anaphase transition is explained by possible regulation of MT binding proteins at both the kinetochore and centrosome.

Materials and Methods

Cell Culture

Porcine kidney epithelial cells of the line LLC-PK (American Type Culture Collection, Rockville, MD) were cultured in DME medium (Sigma Chemical Co., St. Louis, MO) containing 10% fetal bovine serum (Hyclone Laboratories, Logan, UT), 20 mM Hepes, and antibiotics. Two days prior to an experiment, cells were transferred to an etched locator coverslip (Bellco Biotechnology, Bellco Glass, Inc., Vineland, NJ) mounted over a hole in the bottom of a 35 mm culture dish modified for microinjection (Gorbsky et al., 1987) and grown at 37°C in 10% CO_2. Cells from the rat kangaroo epithelial line PtK_1 were cultured similarly but in F-10 medium (Gibco Biological Co., Grand Island, NY) in 5% CO_2.

Preparation of Derivatized Tubulin and Microinjection

Xrhodamine derivatization of tubulin was performed as described previously (Sammak et al., 1987), and the preparation of caged-fluorescein tubulin was essentially as described by Mitchison (1989). The tubulin derivatives were distributed into 5 μl aliquots and stored in liquid nitrogen.

Cells were microinjected according to general protocols as reviewed (Kreis and Birchmeier, 1982). Before microinjection, derivatized tubulin was spun for 30 min at 20,000 *g*, 0°C to clarify the solution and prevent pipette clogging. Micropipettes (WPI, New Haven, CT) were pulled on a vertical pipette puller (David Kopf Instruments, Tujunga, CA). Cells were microinjected using a Nikon Diaphot inverted microscope (Nikon Inc., Garden City, NY) equipped with phase–contrast optics. We generally injected a mixture of xrhodamine tubulin (15 μM) and caged-fluorescein tubulin (120 μM) so that the spindle as well as the activated zone could be visualized. The volume injected was estimated at 5~10% of the cell volume. Cells were microinjected between prophase and metaphase and allowed to incorporate the labeled tubulin subunits into the spindle for at least 20 min before photoactivation and imaging. We found that injected cells showed normal congression and anaphase chromosome movement. After injection, the culture medium was replaced and then overlaid with mineral oil (E. R. Squibb and Sons Inc., Princeton, NJ) to retard gas exchange and evaporation.

Image Acquisition

Instrumentation and experimental procedures for collecting digital fluorescence images were as previously described (Zhai and Borisy, 1994). Photoactivation experiments were performed using the 334–364 nm bands of a 3 W argon ion laser (Spectra-Physics, Mountain View, CA) equipped

with UV transmitting optics, and a Zeiss IM35 inverted microscope with a 100×, 1.3 NA Neofluar objective (Carl Zeiss, Inc., Thornwood, NY). The laser beam was directed into the epi-illumination port while the UV filter cassette was in the light path and aligned with respect to crosshairs. Before photoactivation, the injected cell was located and positioned relative to the laser irradiation beam using phase contrast optics. We verified that the spindle was fully labeled and of normal morphology by observation in the xrhodamine channel prior to activation. A pre-activation image in the fluorescein channel was routinely recorded. The cell was then activated by laser irradiation (30–40 mW) for 30–100 ms. As soon as possible after photoactivation (5–10 s), fluorescence images (0.2–1.0 s) and phase images were collected with a cooled charge-coupled device (model CH220; Photometrics Ltd., Tucson, AZ), and then at 1–3-min intervals. The medium in the culture dish was pre-equilibrated and maintained at the experimental temperature, 23°, 30°, or 37°C, by circulating warm water through a brass block holding the dish chamber and through a coil surrounding the objective during the period of monitoring cells.

Data Analysis

The raw images of fluorescein and xrhodamine fluorescence were adjusted for the nonuniformities in the illumination by flat-field correction as previously described (Zhai and Borisy, 1994). To measure MT turnover, fluorescence intensity values of pixels within a rectangle placed around an activated zone were integrated and computed. Intensity values at successive time points were normalized to the value at zero time and were fitted to a double exponential equation: $I = P_f\exp(-k_f t) + P_s\exp(-k_s t)$; where I = proportion of initial intensity of fluorescence; P_f = proportion of fluorescence decay due to fast process; k_f = rate constant for fluorescence decay (fast process); P_s = proportion of fluorescence decay due to slow process; and k_s = rate constant for fluorescence decay (slow process). Double exponential regression analysis of the data was performed using SIGMAPLOT software (Jandel Scientific, Corte Madera, CA).

Motion of chromosomes and activated zones on kinetochore fibers with respect to the spindle poles was measured using Image-1 software (Universal Imaging Corp.,Westchester, PA). We transferred the charge-coupled device digital images to an OMDR for examination of the movements by rapid playback. The spindle poles were located using the rhodamine fluorescence image. To determine the movements of the activated zones, we measured the distance from the leading edge of the activated zone to the spindle pole. We chose to use the leading edge of the activated zone (as opposed to its midpoint) because the chromosomes nibble away at the trailing edge of the activated zone during anaphase, and thereby artificially shift the mid point of the fluorescent zone poleward. For consistency, we also measured from the leading edge in metaphase cells. Measurements were taken from overlays of the phase, fluorescein and xrhodamine images. Statistical analysis of MT transport data and differences between population averages were calculated with an analysis package (SAS Institute Inc., Cary, NC).

For presentation, images were scaled to 8-bits for display using an Image-1 video processor (Universal Imaging Corp., Westchester, PA). Since the fluorescence intensity of activated zones decreased with time due to the turnover of microtubules, the fluorescein images were digitally adjusted so that their apparent intensity became comparable. This adjustment facilitated subsequent combination with the phase images using a logical max function in order to show their position more clearly. Digital files were recorded with a 4,000 line film recorder, Matrix PCR (Matrix Instruments Inc., Orangeburg, NY), using T-max 100 film (Eastman Kodak Co., Rochester, NY), or printed to a dye-sublimation, Digital Phaser II color printer (Tektronix, Inc., Wilsonville, OR).

Results

Spindle MT Turnover Has Fast and Slow Components

We have quantitatively analyzed MT turnover in metaphase and anaphase using the approach of fluorescence redistribution after photoactivation. LLC-PK and PtK_1 cells in mitosis were microinjected with caged-fluorescein tubulin and allowed to incorporate the labeled subunits into the spindle for at least 20 min before photoactivation and imaging. A typical metaphase cell is shown in Fig. 1 *A* and the absence of fluorescence prior to photoactivation in Fig. 1 *B*. A fluorescent bar was then generated across the MTs in a half-spindle using laser irradiation to uncage the fluorescein (Fig. 1 *C*). As Fig. 1 *C* was obtained 10 s after photoactivation, it also shows an increase in fluorescence throughout the spindle, reflecting the rapid diffusion of soluble tubulin subunits activated in the path of the laser beam (see Discussion). Beyond 10 s, changes in fluorescence intensity primarily reflect MT dynamics. The fluorescence in the marked zone decreased in intensity while the whole spindle became progressively more fluorescent (Fig. 1, *D* and *E*).

The kinetics of fluorescence redistribution were determined as follows. Intensity values of the pixels within a rectangle including the activated zone were integrated and computed (Fig. 1 *D*). The average intensity value obtained from the same size rectangle placed in the opposite half spindle at an equivalent position equidistant from the equator was used as the background value, and subtracted from the activated zone value. Thus, as turnover of labeled subunits within the spindle approaches steady-state, the intensity difference value should ideally approach zero. Quantitative analysis showed that the fluorescence intensity in activated zones decreased rapidly at early times and more slowly at later times, conforming to a double exponential function of time after photoactivation (Fig. 2) with a value for the square of the regression coefficient equal to 0.98.

When the equation for a double exponential curve (see Materials and Methods) is solved, the values of four parameters are obtained: two rate constants and two coefficients; the rate constants (k_f, k_s) for the fast and slow processes and the proportion of fluorescence change (P_f, P_s) that contributes to either the fast or slow process. The turnover half time ($t_{1/2}$) for each process was calculated as ln2/k for each process. The bulk of the fluorescence redistribution after photoactivation at 37°C was rapid. We interpret this rapid dissipation as primarily due to non-kMT turnover because electron microscopic studies have shown that the non-kMTs represent the bulk of MTs within the mammalian cell spindle at 37°C (reviewed in McIntosh et al., 1975; Rieder, 1981*b*). We interpret the more persistent fluorescent zone as reflecting the kMTs, because previous studies have indicated that they may be significantly more stable than non-kMTs (Brinkley and Cartwright, 1975; Salmon et al., 1976, 1984*a*; Rieder, 1981*a*, *b*; Mitchison, 1988; Gorbsky and Borisy, 1989; Cassimeris et al., 1990).

Temperature Dependence of Turnover and Relative Abundance of Spindle MTs

Data sets from cells at lower temperatures also produced double exponential curves but shifted to longer times. A total of 49 metaphase LLC-PK cells maintained at 37°, 30°, or 23°C were analyzed. A fast and slow process was identified by quantitative analysis of the data sets at each of the temperatures (Fig. 3 *A*). Within the error of the data, statistically significant changes in the fast process (non-kMTs) were not detected. However, the slow process (kMTs) showed a pronounced temperature dependence. At 37°C, the turnover of kMTs was almost twice as fast as that at 30°C, and more than three times as fast as that at 23°C. The turnover of kMTs in 17 metaphase cells of a dif-

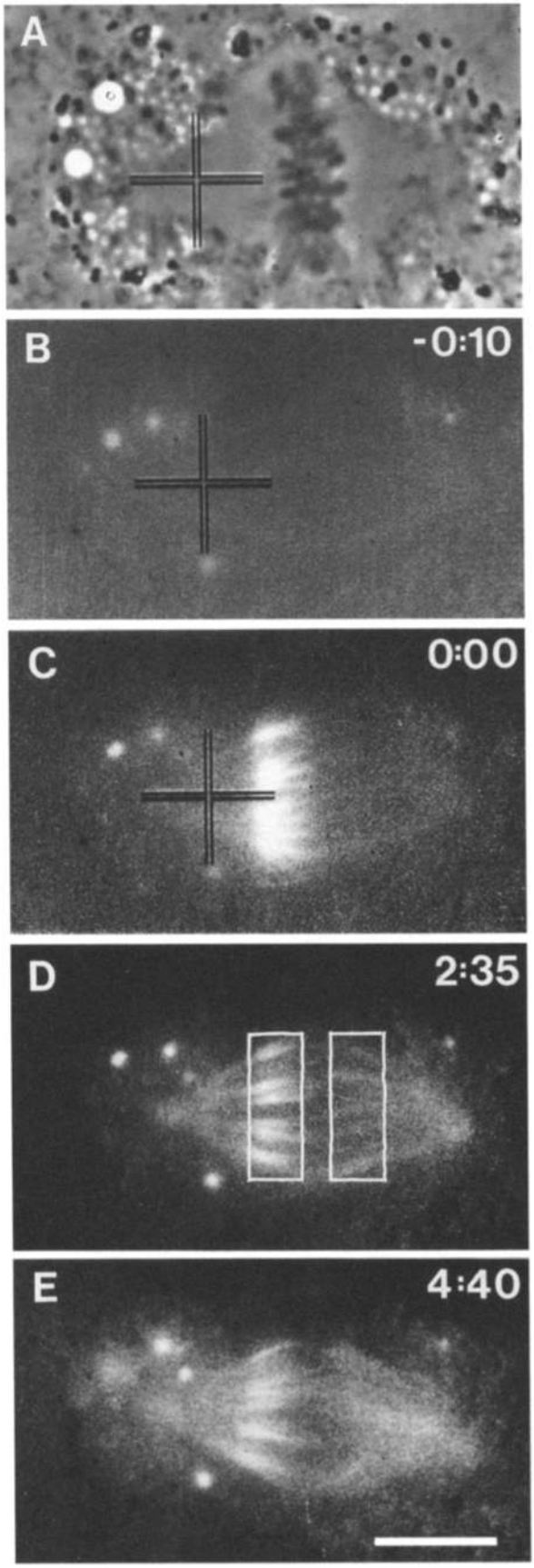

Figure 1. Photoactivation in metaphase. (*A*) shows phase contrast image of the metaphase spindle and (*B*) shows a fluorescence image in the fluorescein channel prior to photoactivation. (*C*) shows a fluorescent bar that was generated across the MTs in a half-spindle using laser irradiation at time 0. The loss of fluorescence intensity in the bar, i.e., turnover of spindle MTs can be observed in panels (*D* and *E*). Initially the MTs turnover at a very fast rate so that at 2:35 min most of the labeled subunits from the activated zone have become redistributed throughout the spindle (*D*). Between 2:35 min and 4:40 min, the fluorescent subunits continue to be lost from the activated bar but at a slower rate. Bar, 10 μm.

ferent cell line, PtK_1, was also measured at 37°C using the same technique. The turnover half-time was 0.68 ± 0.4 min for the fast component, and 5.3 ± 0.8 min for the slow component, similar to the result obtained for LLC-PK cells.

We were concerned that some of the apparent decrease in fluorescence was due to bleaching of the fluorescein, and that this introduced error in the determination of turnover times. The bleaching rate was measured using fluorescein labeled spindles and was found to be 3.9% per second of exposure with a 100 × 1.3 NA objective under our standard observation conditions. Most of our exposures to collect data for turnover were less then one second (see Materials and Methods), and when the data were corrected for the bleaching effect, the turnover $t_{1/2}$ did not change significantly compared with the uncorrected data (not shown). Therefore, the slow process of fluorescence decay was not due to bleaching.

The double exponential analysis of the temperature data also gives parameters for the proportions of the fast and slow processes contributing to the overall fluorescence dissipations (Fig. 3 *B*). These parameters may be equated to the relative abundance of non-kinetochore and kMTs within the spindle. At normal growth temperature (37°C), the fast process accounted for 74% of the fluorescence intensity change and, therefore, we infer that non-kMTs accounted for 74% of all spindle MTs. With lower temperatures, this proportion decreased, reaching 39% at 23°C, a temperature at which cells were still able to progress through mitosis. Conversely, the slow process accounted for 26% of the fluorescence intensity change, indicating that kMTs make up only 26% of all spindle MTs at 37°C. With lower temperature, this proportion increased, reaching 61% at 23°C. These proportions are reasonably consistent with the results obtained from electron microscopic studies (Rieder, 1982; Cassimeris et al., 1990; Wise et al., 1991). These results also indicate that the non-kMTs are normally present in excess since much lower numbers are sufficient to achieve mitosis.

kMT Turnover at the Metaphase–Anaphase Transition

We also performed photoactivation analysis of MT turnover in anaphase cells essentially as described for metaphase except that cells were injected in metaphase and allowed to progress to anaphase before photoactivation. Fig. 4 shows a typical example of an anaphase experiment. Fluorescence dissipation in the activated zones was assayed and the data were then fitted to a double exponential curve (Fig. 5) as described previously. As for metaphase, fast and slow processes were identified by the kinetic analysis. The turnover half-time, $t_{1/2}$, and the relative propor-

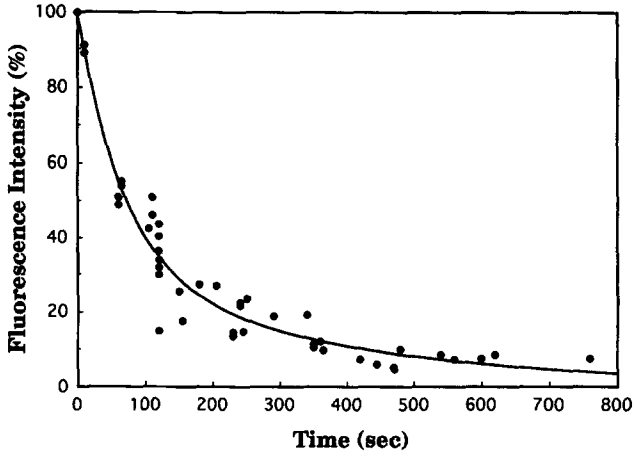

Figure 2. Dissipation of fluorescence after photoactivation in metaphase. The filled circles plot the loss of fluorescence from the activated zone of spindles at 37°C. The line was generated by a non-linear curve fitting program with a double exponential equation. The best fit for this fluorescence loss data turns out to be a double exponential curve. The graph shows that the fluorescence decreases at a rapid rate at early times and at a slower rate at later times. A total of 15 cells were analyzed and 58 data points were generated to plot this graph. At time 0, fluorescence intensities were considered to be 100%; therefore, the zero time point represents 15 data points. When the equation for the double exponential curve is solved, the rate constants as well as the percentage of MTs for the fast and slow process are obtained.

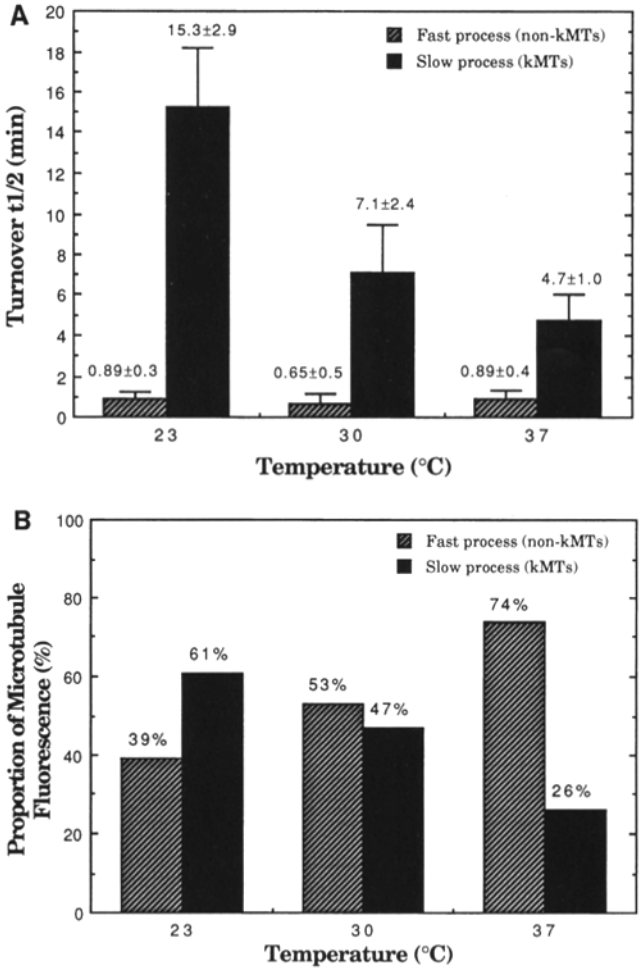

Figure 3. Turnover and the relative proportion of spindle MTs in metaphase. (*A*) The turnover half time for the spindle MTs at three temperatures is shown in histogram form. The turnover half time for each process was derived from the respective rate constant of the double exponential equation. The striped histograms represent the fast process and the filled histograms represent the slow process. The data indicate that kMTs turn over more slowly at lower temperatures. (*B*) The proportion of kMTs and non-kMTs at each temperature was derived from the P_s and P_f parameters of a double exponential equation. The composition of the spindle at each temperature is shown in the accompanying histograms. The proportion of non-kMTs in the spindle decreases with decreasing temperature.

tions, P_f, P_s, for the fast process (non-kMTs) and the slow process (kMTs) in anaphase was determined at 37° and 30°C (Table I).

Comparison of the kinetics of fluorescence dissipation in metaphase and anaphase showed significant similarities and differences. Both phases of mitosis showed similar temperature dependence of kinetic parameters. Turnover half-times of kMTs increased 1.5-fold for metaphase and 1.7-fold for anaphase when the temperature was reduced from 37°–30°C. Similarly, the proportion of kMTs increased by similar differentials; 19% (from 26–47%) in metaphase and 18% (from 45–63%) in anaphase. Metaphase and anaphase cells were also similar in terms of the fast process not showing detectable dependence on temperature.

The differences between metaphase and anaphase were in the absolute values for turnover half-time and the proportion of the slow process. In anaphase, the turnover was approximately fivefold slower than in metaphase, over the range of temperatures examined. In addition, the slow process accounted for a greater proportion of the total fluorescence change than in metaphase (e.g., 45 vs. 26% at 37°C). At first, it may seem anomalous that a higher proportion is attributed to kMTs in anaphase, a stage where it is clear that they are depolymerizing. However, the bar photoactivation approach, strictly speaking, provides a measure of tubulin distribution only in the region of activation. In anaphase, astral MTs elongate and interzonal MTs form. Since we have shown (Zhai and Borisy, 1994) that mitosis proceeds under the constraint of essentially constant MT polymer levels, we interpret the higher value for the proportion of kMTs to mean that subunits from the more labile non-kMTs in the region of photoactivation have re-equilibrated to sites of polymerization outside the region. This interpretation is supported by several electron microscopic studies that have shown a significant decrease in the total number of MTs in this spindle area in anaphase compared to metaphase (Brinkley and Cartwright, 1971, 1975). If the number of kMTs is constant and the number of non-kMTs decreases in anaphase then the proportion of kMTs in this region becomes larger just as our fluorescence data indicates.

To further investigate the shift in the turnover of kMTs at the metaphase–anaphase transition, and whether the turnover rate changed gradually or rapidly from metaphase to anaphase, we measured MT turnover in meta-

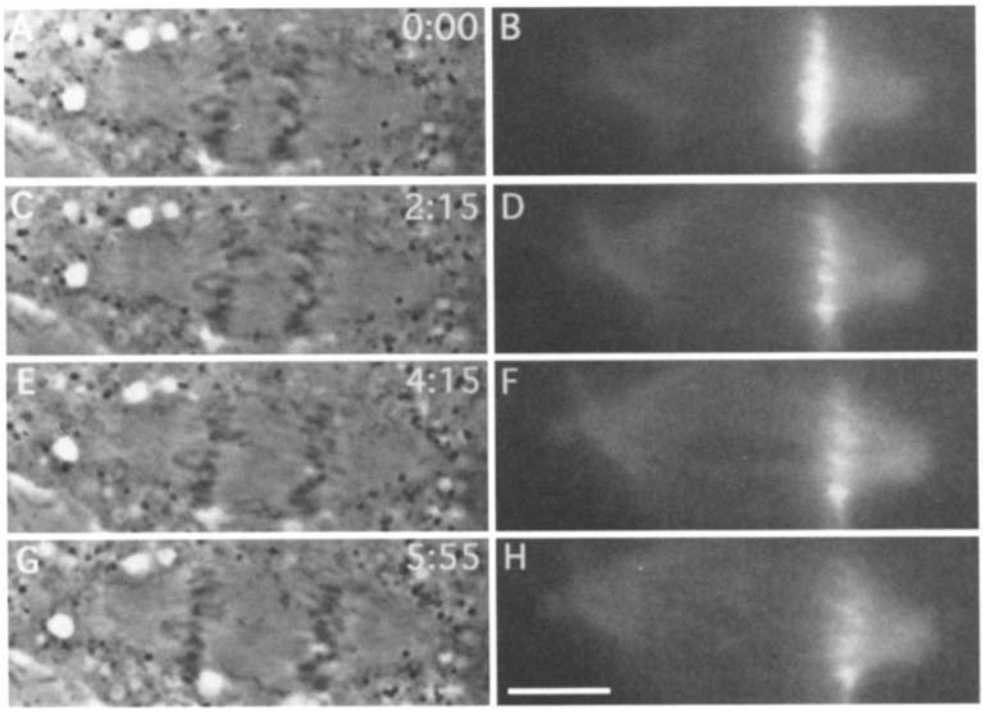

Figure 4. Photoactivation in anaphase. An LLC-PK cell was microinjected at metaphase with a mixture of caged-fluorescein tubulin and xrhodamine tubulin and, then, after anaphase onset, a bar of U.V. light was used to generate a fluorescence zone across the MTs in a half-spindle at time 0. (*A*, *C*, *E*, and *G*) show phase contrast images of the anaphase spindle and (*B*, *D*, *F*, and *H*) show fluorescence images after photoactivation. The loss of fluorescence intensity in the bar, i.e., turnover of spindle MTs, was measured as described for metaphase. The activated zone was placed about 3–5 μm away from the kinetochore. This cell was observed at 30°C. Xrhodamine images were used to image total spindle MTs (not shown). Bar, 10 μm.

phase and anaphase using a double photoactivation procedure in the same cells. We microinjected either prophase or metaphase cells with caged-fluorescein tubulin and an activated bar was introduced across the metaphase spindle as previously described. After anaphase onset, a second activated zone was introduced across the other half spindle. Since in most of the cells, the activated bars were generated several micrometers away from chromosomes, we had enough time to take multiple fluorescence images before the chromosomes translocated through the activated bar as they depolymerized the kMTs and progressed poleward.

The turnover $t_{1/2}$ for kMTs was determined at metaphase and anaphase in the same cells as described previously for separate cells in either metaphase or anaphase. 15 such cells were analyzed and the $t_{1/2}$ for kMTs was 6.4 ± 1.2 min in metaphase, and 35.5 ± 5 min in anaphase. This 5.5 fold slowing of kMT turnover from direct analysis of the metaphase-anaphase transition in single cells confirms the conclusions drawn previously from an analysis of separate populations of metaphase and anaphase cells. We also compared the data obtained from early metaphase cells (12 min before anaphase onset) with the data obtained from later metaphase cells (3 min before anaphase onset), and found the turnover $t_{1/2}$ to be similar at both times. These results demonstrate an abrupt slowing of kMT turnover at the metaphase–anaphase transition.

Poleward MT Transport in Metaphase and Anaphase

To investigate the possible regulation of poleward MT transport at the metaphase-anaphase transition, conditions had to first be established for routinely observing the transport. Our initial photoactivation experiments were conducted at 37°C, the normal growth temperature for these cells. At this temperature, no transport was detectable with confidence; instead, we saw rapid dissipation of the fluorescence after photoactivation, presumably by turnover (Fig. 1). The fluorescence signal in the activated zone fell while the signal in the balance of the spindle rose, precluding any determination of whether transport

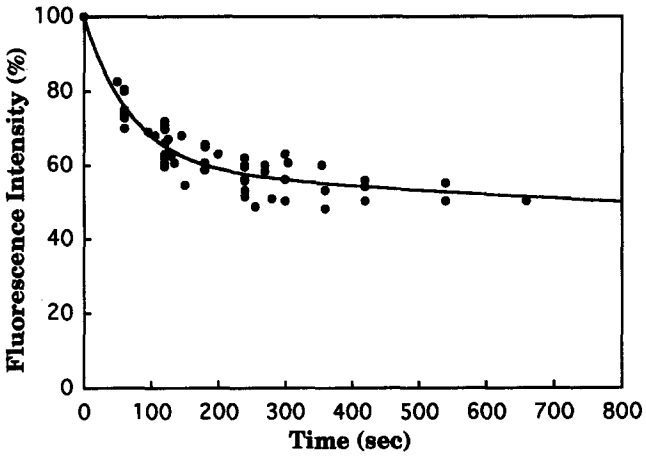

Figure 5. Fluorescence dissipation after photoactivation in anaphase. The filled circles plot the loss of fluorescence from the activated zone of anaphase spindles at 30°C. The line was generated by a non-linear curve fitting program with a double exponential equation. The graph shows that, after an initial drop, the fluorescence decreased slowly through anaphase. A total of 14 cells were analyzed. Fluorescence intensities at time 0 were considered to be 100%. The turnover half time and the proportion of spindle MTs for each process were derived from the respective rate constants and coefficients obtained as described for metaphase.

Table I. Turnover and Proportion of Spindle MTs

Experimental condition	Turnover time	Proportion
	$t_{1/2}$ min	P_f, P_s %
A. Metaphase		
37°C (fast process)*	0.9 ± 0.4	74
(slow process)‡	4.7 ± 1.0	26
30°C (fast process)	0.7 ± 0.5	53
(slow process)	7.1 ± 2.4	47
B. Anaphase		
37°C (fast process)	1.0 ± 0.5	55
(slow process)	22.4 ± 4.8	45
30°C (fast process)	1.2 ± 0.6	37
(slow process)	37.5 ± 8.5	63

The results obtained from a total of 35 cells in metaphase at 30° and 37°C are shown in A. (*B*) shows the results obtained from a total of 26 anaphase cells. The turnover time and the relative proportion of spindle MTs were obtained from a double exponential analysis. We interpret the fast process as being non-kMTs and the slow process as being kMTs (see text). Comparison of the results in metaphase and anaphase showed significant similarities and differences. We conclude that there is a dramatic shift in MT dynamics within the spindle from metaphase to anaphase.

*Fast process, non-kMTs.

‡Slow process, kMTs.

had occurred in addition to the turnover. For transport to be observable, the activated zone has to move a significant distance (its width) before the fluorescence of the zone is too dissipated (a function of its half-time). For example, if the zone is 3-μm wide and the half-time for turnover is 4 min, and then one may calculate that transport would need to occur at about 0.75 μm/min for it to be readily observable.

The turnover by fluorescence dissipation experiments reported here permitted us to quantitatively evaluate the relative proportions of kMT and non-kMTs as well as the dependence of their turnover on temperature. Lower temperatures provided the combined advantages of slower turnover and a reduced proportion of non-kMTs. Thus, the window of observation for transport could be extended both in terms of rate and signal-to-noise.

In the photoactivation marking experiments described here, cells were maintained at 23° or 30°C during the observations. At these temperatures, although the process of mitosis was somewhat slower than at 37°C, spindle morphogenesis and chromosome segregation were otherwise normal. We first studied MT transport in metaphase and anaphase separately. Fig. 6 shows an LLC-PK metaphase cell, microinjected with a mixture of caged-fluorescein tubulin and xrhodamine tubulin, and then activated at metaphase with a bar of UV light. The rhodamine channel (Fig. 6, *A* and *F*) shows that the morphology of the spindle was normal; these images were used to determine the positions of the poles in order to accurately assess poleward movement. Phase images were used to determine the positions of the chromosomes and where to place the activated zone, the timing of which was defined as time 0 (Fig. 6 *B*). An intensity trace through the activated zone gave its width at half-maximum to be 2.8 ± 0.5 μm (n = 11). The juxtaposition of the phase and fluorescence images (Fig. 6, *B–E*) shows clearly the poleward movement of the activated zone occurring throughout metaphase. Anaphase onset (Fig. 6 *G*) occurred normally and the cell progressed through telophase and cell division.

To assess poleward transport in anaphase, we microinjected LLC-PK cells at metaphase with a mixture of caged-fluorescein and xrhodamine tubulin as before, and waited for the cells to enter anaphase. Cells were monitored by phase microscopy to keep the total fluorescence exposure low. Upon anaphase onset, a fluorescent mark was generated across the spindle MTs using laser irradiation as described for metaphase. To measure the rate of poleward movement of the marked zone in both metaphase and anaphase cells, the distance between the spindle pole and the leading edge of the marked zone was measured. The leading edge, as opposed to the midpoint, was chosen for consistency, because the chromosomes gradually consume the trailing edge of the activated zone during anaphase, thus shifting the midpoint poleward. Only those cells where the position of the near pole was unambiguously located in either the rhodamine or fluorescein channel were used for analysis. In addition to the movement of the activated zone, we also measured chromosome movement and spindle elongation. The results demonstrate by the photoactivation approach the same conclusion first established through the photobleaching approach (Gorbsky et al., 1987, 1988); namely, that the loss of MT subunits occurs primarily at the kinetochore during anaphase as chromosomes approach and pass through the marked zone.

Observations were made on cells in metaphase or anaphase to build up the sample size and obtain values for the rates of movement (Table II). Movement plots of activated zones for 16 metaphase cells at 30°C gave an average rate of 0.39 ± 0.20 μm/min, and for five metaphase cells at 23°C a rate of 0.45 ± 0.15 μm/min. The difference in rate between the two temperatures is not statistically significant. The average rate of the movement of the activated zones for 11 anaphase cells was 0.2 ± 0.1 μm/min, significantly different from the metaphase values as evaluated by an analysis of variance model. The poleward MT transport in PtK_1 cells was also measured at 30°C using the same technique and found to be similar to the result obtained for LLC-PK cells. Thus, poleward transport of MTs in anaphase occurs at approximately half the rate seen in metaphase.

Abrupt Change of MT Transport at the Metaphase-Anaphase Transition

Our analysis of populations of metaphase and anaphase cells suggested that poleward MT transport was reduced in anaphase to approximately half that of metaphase. However, the in-group variance for each population was large, thus reducing the strength of the conclusion that the two populations differed. Further, the population analysis was unable to address the question of whether the change in transport developed gradually as anaphase progressed or occurred suddenly at the metaphase-anaphase transition. To gain better precision in the determination of poleward transport and to evaluate whether the slowing in anaphase was gradual or abrupt, we performed double photoactivation analyses on single cells as previously described.

In these double activation experiments, we normally took four to six fluorescein images during metaphase as the cells progressed toward anaphase and then an additional four to six images after anaphase onset. Fig. 7 shows a typical sequence in which a mark was generated across

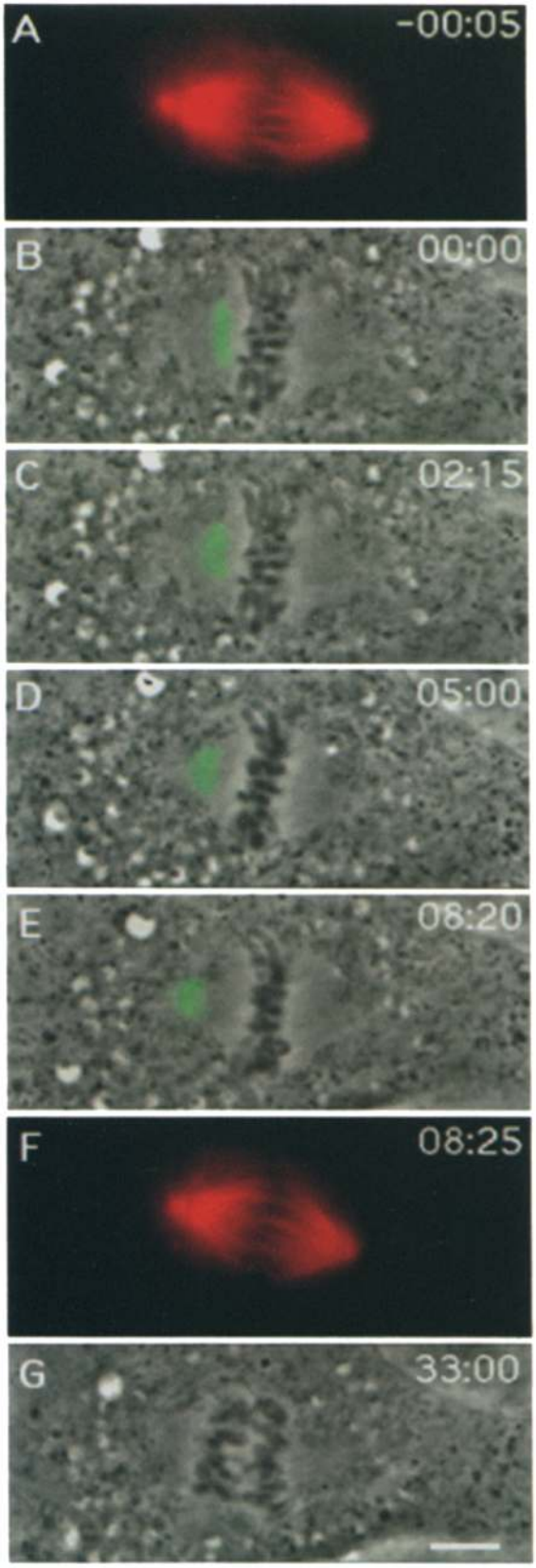

Figure 6. Overlay of fluorescence and phase contrast images showing the movement of an activated zone in a metaphase cell (*B–E*). The top (*A*) and bottom (*F*) panels show the rhodamine MT images of the spindle taken at the beginning and end of the series. An activated zone was introduced at time 0 (*B*). During the following 8:20 min the zone of fluorescein fluorescence moves toward the left spindle pole. The movement of the fluorescent zone indicates the poleward movement of tubulin subunits in the spindle during metaphase. The activated bar introduced in this metaphase cell moved poleward at a average rate of 0.52 μm/min. The panel (*G*) shows the cell started a normal anaphase at time 33 min. Bar, 10 μm.

Table II. Poleward Microtubule Transport

Experimental condition	Metaphase (mean ± SD)	Anaphase (mean ± SD)
	μm/min	*μm/min*
A. LLC-PK cells		
30°C population analysis	0.39 ± 0.20 (n = 16)	0.20 ± 0.1 (n = 11)
30°C same cell analysis	0.37 ± 0.23 (n = 14)	0.19 ± 0.1 (n = 14)
23°C population analysis	0.45 ± 0.15 (n = 5)	
B. PtK_1 cells		
30°C population analysis	0.46 ± 0.14 (n = 10)	0.21 ± 0.1 (n = 3)

Comparison of kMT movement at the metaphase–anaphase transition. The movement of poleward MT movement in metaphase and anaphase cells were analyzed in a population and in the same cells (see text). The slope of the least-squares fit gave a rate of kMT movement with a 95% confidence interval. The results obtained from both population and same cell analysis show that kMT movement reduces significantly at the metaphase–anaphase transition.
n, number of cells.

one half of the metaphase spindle at time 0, and a second mark was then generated in the other half spindle after anaphase onset at time 6:20 min. The double photoactivation and the onset of anaphase allowed two comparisons to be made: (*a*) comparison of the movement of a zone activated in metaphase to one activated in anaphase gave a direct measure of possible differences in transport properties in the two phases of mitosis; (*b*) comparison in anaphase of the new zone (established in anaphase) to the old zone (established in metaphase) provided an internal control to assess whether the transport properties displayed by the zones were dependent on the history of their creation and observation.

To quantitate the poleward MT transport, the positions of the poles, chromosomes and the activated zones were determined as described previously and movement plots were generated. In Fig. 8, linear least square regression analysis yielded a metaphase MT transport rate for this cell (Fig. 7) of 0.54 μm/min, an anaphase rate of 0.17 μm/min for the first activated zone (introduced in metaphase), and an anaphase rate of 0.20 μm/min for the second activated zone (introduced after anaphase onset). The equivalence in the anaphase transport rates for the first and second activated zones supports the conclusion that the behavior of the zones is reflecting intrinsic spindle MT dynamics and is not an artifact of the double photoactivation procedure. The change in slope at the time of anaphase onset supports the conclusion that the MT transport properties change abruptly at the metaphase-anaphase transition. As a measure of the magnitude of the slowing, the metaphase rate (M) was computed as a multiple of the anaphase rate (A) for those cells in which a sufficiently clear data set was collected in both phases to permit the comparison. For the cell in Figs. 7 and 8, the ratio, M/A was 3.2. An additional four cells showed similar patterns

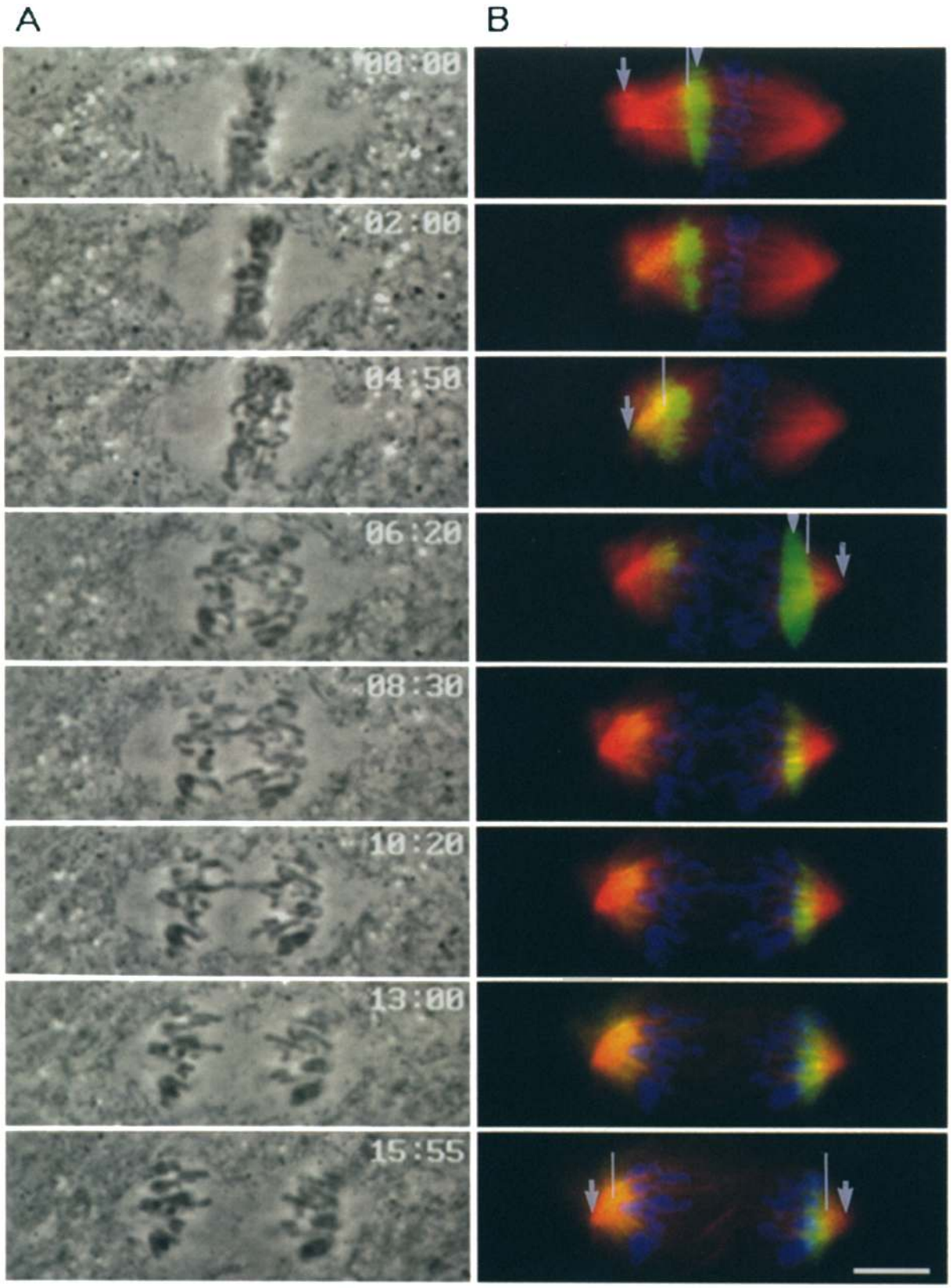

Figure 7. Shift in MT movement at the metaphase-anaphase transition measured in a single LLC-PK cell. Phase, fluorescein, and xrhodamine fluorescence images were taken over a 16 min time period. (*A*) shows phase contrast images, (*B*) shows chromosomes superimposed on the fluorescein–xrhodamine composite. An activated zone was generated in metaphase spindle at time 0. A second activation zone was introduced after anaphase onset at 6:20 min. The arrows indicate the position of the spindle pole which was positioned by xrhodamine fluorescence images. The leading edge of the activated zone is indicated by the white lines, and the center of the activated zone by the arrow heads. Bar, 10 μm.

and gave M/A ratios of 2.8, 2.2, 3.4 and 3.9. A total of 14 cells were double photoactivated and provided data that could be analyzed in the aggregate (Fig. 9), yielding an average metaphase movement of 0.37 ± 0.23 μm/min and an average anaphase movement of 0.19 ± 0.1 μm/min. Statistical comparison of population analysis and same cell analysis was made as described above, and indicates that there was no significant difference between the population analysis and same cell analysis. We conclude that the poleward movement occurring in metaphase slows abruptly at anaphase onset.

In comparison with poleward MT transport in anaphase, poleward transport of chromosomes occurred significantly faster. The speed of chromosome movement is not uniform throughout anaphase but, rather, is faster in early anaphase and slows as anaphase progresses. Over the first five minutes of anaphase, poleward chromosome movement in LLC-PK cells occurred at an average rate of 1.15 ± 0.15 μm/min, a value approximately sixfold greater than the rate of MT transport over this same time period. In terms of distances, MT transport accounted for only 1 μm of movement or less than 20% of the total chromosome movement over this period. In contrast, in late anaphase (beyond five minutes), chromosome movement toward the pole slowed to an average rate approximating that of MT transport. Thus, two activities are involved in the poleward motion of chromosomes and their relative proportion changes as anaphase progresses. Over the entire course of anaphase, poleward MT transport accounted for approximately 33% of the total chromosome movement.

Finally, we have evaluated MT turnover and transport in interphase cells using the same approach (data not shown). Random interphase cells were microinjected, tubulin was allowed to incorporate for 2 h and then an activated zone was generated across the MTs either near the centrosome or at the periphery of the cell. A total of 38 cells were analyzed and we found that the $t_{1/2}$ for MTs was 5.75 ± 1.8 min in interphase cells. To measure MT transport, we measured the distance between the proximal edge of the activated zone and the centrosome as described above. We considered whether the degree or lack of transport depended upon the orientation of the zone or its distance from the centrosome. Comparison studies with zones in different orientations with respect to the primary direction of microtubules either near the centrosome or at the periphery of the cell gave essentially identical results. We found no MT movement toward the centrosome in interphase, in contrast to the behavior in mitotic cells.

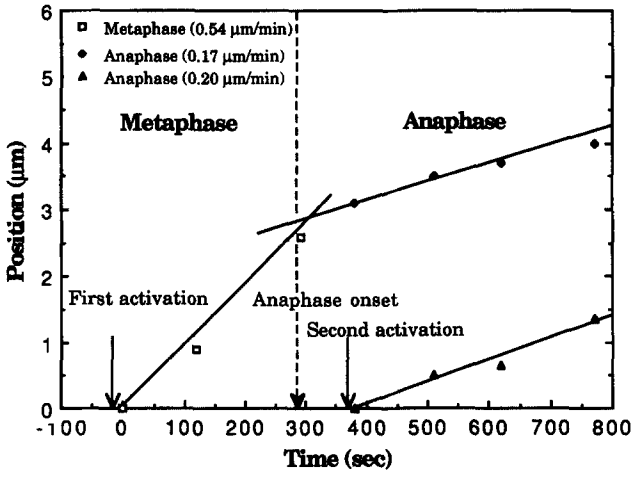

Figure 8. Graph showing the poleward movement of the activated zones in the cell shown in Fig. 7. The first activation was made in a metaphase spindle at time 0. The cell entered anaphase at approximately 4:50 min. A new activation zone was introduced at time 6:20 min. Linear least square regression lines are drawn through the data points. Open squares show that the activated zone introduced in metaphase moved poleward at a rate of 0.54 μm/min during metaphase. After the onset of anaphase this same zone moved poleward at a rate of only 0.17 μm/min shown by filled circles. Triangles show that the bar introduced in anaphase moved at a similar rate of 0.20 μm/min.

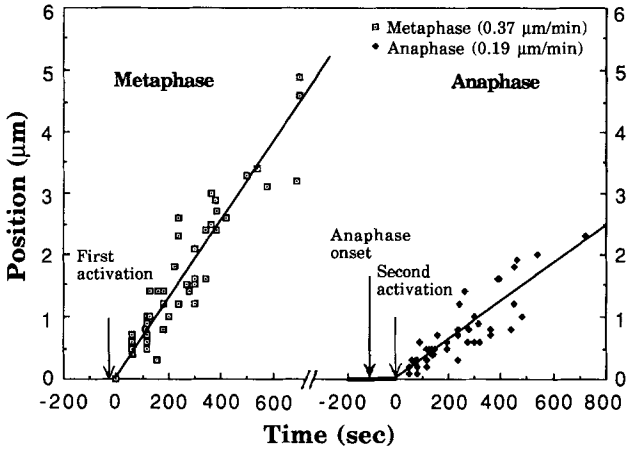

Figure 9. Comparison of metaphase movement and anaphase movement in a population of twice activated cells. This figure plots the movements of an activated zone introduced in a metaphase spindle at time 0, and of a second activated zone introduced in an anaphase spindle after anaphase onset. The movements of activated zones were measured in a total of 14 cells and 82 measurements were made and plotted. The slope of the least-squares fit gave a rate of kinetochore MT movement of 0.37 ± 0.23 μm/min in metaphase and 0.19 ± 0.1 μm/min in anaphase cells with a 95% confidence interval.

Discussion

kMT Turnover in Mitotic Spindle

The major focus of the experiments presented here is a quantitative analysis of kMT turnover and transport together with changes in their dynamic behavior at the metaphase-anaphase transition. We will discuss these two aspects of kMT dynamics in turn. By using fluorescence dissipation after photoactivation as an experimental approach and by modeling spindle MT turnover as a double exponential system consisting of fast and slow processes, we have operationally distinguished the contributions of the non-kMTs from the kMTs. Based on the diffusion coefficient of tubulin and the viscosity of cytoplasm, the diffusion of tubulin subunits out of the narrow activated zone would have an estimated $t_{1/2}$ of 5–10 s (Wojcieszyn et al., 1981; Salmon et al., 1984*b*; Pepperkok et al., 1990) and,

thus, be substantially completed by the time our first image was taken 10 s after photoactivation. Therefore, the fast process in our analysis reflects primarily non-kMT turnover and not diffusion. On the assumption that turnover of non-kMTs dominates spindle dynamics under standard experimental conditions, our results are consistent with photobleaching studies which reported that spindle MTs turn over very rapidly ($t_{1/2}$ = 15–80 s) (Salmon et al., 1984*b*; Saxton et al., 1984; Wadsworth and Salmon, 1986; Hamaguchi et al., 1987; Cassimeris et al., 1988; Gorbsky et al., 1990; Hush et al., 1994). Similar to the results obtained from the photobleaching studies, we found that the turnover $t_{1/2}$ for non-kMTs in both metaphase and anaphase spindles was approximately 1 min. Comparable values were obtained at the different temperatures investigated. However, due to the limited number of early time points in our experiments, we can not exclude the possibility that the behavior of non-kMTs does vary with temperature, and this point will require data of higher temporal resolution. Similarly, we cannot exclude the possibility that turnover of non-kMTs might be significantly slower in anaphase than it is in metaphase.

Our results clearly establish the existence of a slow process of MT turnover and we infer from these results that kMTs turn over in metaphase more slowly ($t_{1/2}$ = 4.7 min at 37°C) than previously thought from photobleaching studies, and become still slower in anaphase ($t_{1/2}$ = 22.4 min at 37°C). However our long half lives for kMTs are similar to those obtained using nocodazole induced depolymerization and correlative electron microscopy (Cassimeris et al., 1990). Since many kMTs run continuously between the kinetochore and the pole (Rieder, 1981*a*; McDonald et al., 1992) and they are more stable than non-kMTs, it is likely that their enhanced stability is a consequence of their interaction with the kinetochore. However, it should be noted that the EM MT tracking studies also show that not all MTs in the kinetochore fiber attach to the kinetochore. Many of these are probably intermingled non-kMTs and could be included in our fast turnover class.

The mechanism of kMT turnover can be accounted for by a cycle of detachment of MTs from the kinetochore, depolymerization, repolymerization, and reattachment (Fig. 10 *A*). Once kMTs detach from the kinetochore, there is evidence that they are indistinguishable from non-kMTs and may depolymerize completely or partially (Nicklas and Kubai, 1985; Spurck et al., 1990; Czaban et al., 1993). Subsequently, the same MT or a new MT may regrow and be captured by the kinetochore (Mitchison and Kirschner, 1985*a*,*b*; Huitorel and Kirschner, 1988; Wise et al., 1991). This idea of a cycle of release and capture of MTs by the kinetochore suggests that the turnover of kMTs is limited by the rate constant, k_r, for their release. On the assumption that shrinking and regrowth are fast, the overall turnover of MTs in a kinetochore fiber would be determined by the kinetics of release which can be modeled as an exponential decay process with $t_{1/2} = \ln 2/k_r$. From our estimate that non-kMT turnover has a half-time of 0.9 min at 37°C, we calculate that kMTs in metaphase spend approximately 80% of their time attached and 20% detached from the kinetochore. In a metaphase kinetochore fiber consisting of 25 MTs, this would mean that at any given time, on average, 5 of the kMTs are detached and subject to turnover while the remaining 20 maintain the structural integrity of the fiber.

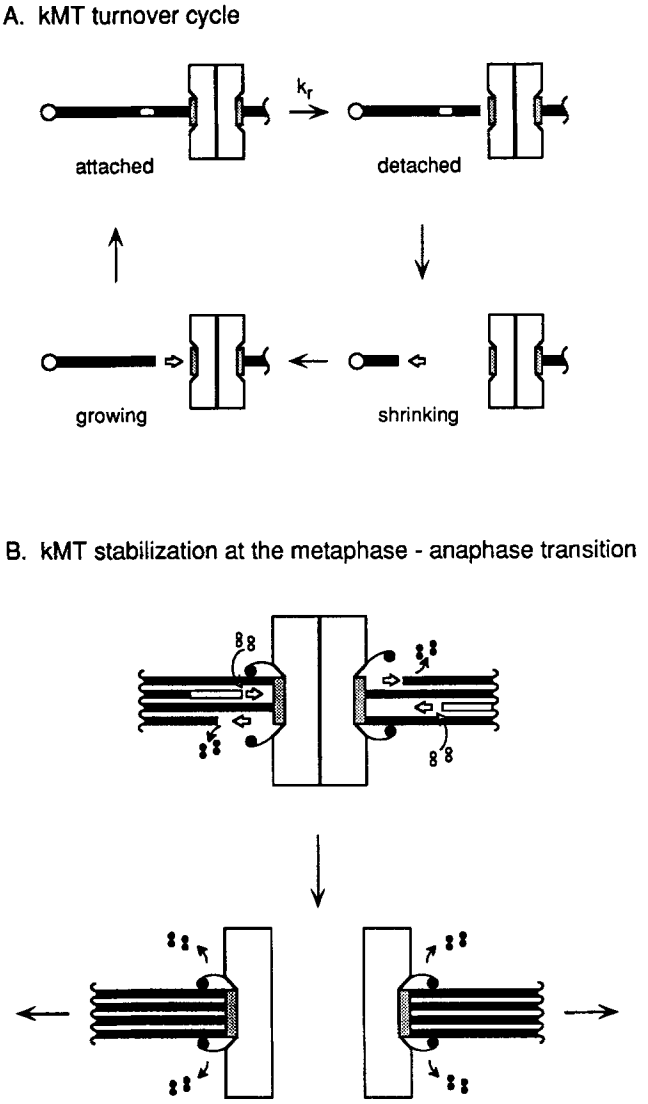

Figure 10. Diagram of the mechanism of kMT turnover. (*A*) shows a four-step kMT turnover cycle where k_r is the rate constant for detachment of kMTs. The filled bars represents individual kMTs and the open segment represents a zone of photoactivation. Once a kMT is released from the kinetochore, it may depolymerize completely or partially and subsequently regrow and be captured by the kinetochore. This cycle continues during the course of chromosome congression and oscillation. (*B*) shows kMT stabilization at the metaphase–anaphase transition. Here, open segments represent newly formed MTs. The stability of kMT attachment to the kinetochore is modulated by MT binding protein(s) at the kinetochore. In metaphase, kinetochore proteins loosely bind to MTs, thus frequently allowing kMTs to detach, while in anaphase strong binding reduces kMT detachment.

In anaphase, one may calculate that the kMTs would spend >95% of their time attached. Since in PtK_1 cells the average number of kMTs does not change significantly from metaphase to anaphase (McDonald et al., 1992), this

means that over the normal 10 min course of anaphase, less than 6 MTs (out of 25 per kinetochore) would detach. This quantitative analysis agrees with the stability of anaphase kMTs reported previously (Gorbsky and Borisy, 1989) and is also consistent with the persistence of photobleached zones in anaphase cells observed in our original studies on localizing the site of kinetochore fiber depolymerization (Gorbsky et al., 1987, 1988). Although the release–capture model predicts that MT detachment from the kinetochore in anaphase is rare, it does not preclude addition of subunits under conditions of high pool concentrations of tubulin. Thus, our conclusions are not inconsistent with studies showing injected tubulin incorporating into kMTs during early but not late anaphase (Wadsworth et al., 1989).

Our results have also demonstrated a significant temperature dependence for the turnover of kMTs with the turnover $t_{1/2}$ decreasing at lower temperature. The greater stability of kMTs at lower temperature may reflect the thermodynamics of the interaction between MTs and the kinetochore. As temperature drops, kinetochore proteins may release their hold on kMTs less frequently. Another possibility may be that at lower temperatures, since there are fewer non-kMTs to bind the MT-associated proteins (MAPs), the remaining kMTs may become more saturated with stabilizing MAPs and depolymerize more slowly and less frequently.

kMT Turnover and the Metaphase-Anaphase Transition

The dramatic shift in kMT turnover from metaphase to anaphase raises questions as to its mechanism and biological significance. The successful segregation of chromosomes requires stable connection to the poles. However, in prometaphase, chromosomes frequently make errors in their attachment which are subsequently corrected, suggesting that dynamic kMTs may be very important at this stage for correcting malorientations. The question, then, is how the cell contrives to insure moderately dynamic kMTs in metaphase but stable ones in anaphase.

One possible explanation for the reduced turnover of kMTs in anaphase may be a change in the intrinsic dynamic behavior of kMTs. Since anaphase onset marks the beginning of a return of many cellular processes to the interphase state (Murray and Hunt, 1993), it seems reasonable to assume that the dynamic behavior of kMTs might change from metaphase to anaphase. According to this view, released kMTs would not be prone to the rapid depolymerization seen in metaphase, and the measured turnover of anaphase kMTs would be slower than at metaphase even if the release rate were the same. However, the observation that severed anaphase kMTs depolymerize poleward just as they do in metaphase (Spurck et al., 1990) argues against this explanation.

Alternatively, on the assumption that the release–capture model given above approximates the mechanism of kMT turnover, the release step would be rate-limiting and a change in dynamic behavior could be interpreted in terms of modifications to the kinetochore that effect kMT release (Fig. 10 *B*). Binding of MTs to the kinetochore could be affected by the affinity of motors, MAPs or as yet unidentified kinetochore proteins. The simplest model to account for the increased stability of kMTs at the metaphase-anaphase transition would have the kMT binding proteins modified at the metaphase–anaphase transition to reduce the probability of MT release. A variation of this model is also worth noting.

During prometaphase and metaphase, chromosomes undergo oscillations with frequent switches between states of moving towards and away from a spindle pole (Skibbens et al., 1993). It is possible that the kinetochore proteins that bind to the kMTs during MT shortening (possibly minus end–directed motors) are different from those that bind to the kMTs when the MTs are growing (possibly plus end–directed motors). If the proteins responsible for binding to the shortening kMTs bind tightly, whereas the proteins that hold the kMTs during the elongation phase frequently release individual MTs and allow them to be replaced, then the difference between metaphase and anaphase kMT turnover can be explained. Metaphase measurements would include kMTs that were switching between growing and shortening states, with all entering the labile growing state at some time during the measurement period. By contrast, most of the kMTs in anaphase would be tightly bound to their kinetochores in a continuous shortening state which only rarely switches to a growing phase (Skibbens et al., 1993). This mechanism would predict that even in metaphase the leading kinetochore fiber of a moving chromosome would be less dynamic then the trailing kinetochore fiber. Though technically difficult, this prediction could be tested experimentally. Irrespective of the details, our results suggest that regulation at the level of the kinetochore is involved in increasing the stability of chromosome attachment and insuring the fidelity of segregation.

MT Transport and the Metaphase-Anaphase Transition

Our previous photobleaching studies of mitotic cells (Gorbsky and Borisy, 1989) were consistent with a slow poleward translocation of kMTs, although the large variation in the data precluded a strong conclusion on this point. The variation was probably due to technical limitations imposed by the lower signal-to-noise ratio inherent in the photobleaching approach, fairly rapid turnover of kMTs at 37°C (for discussion of kMT turnover see Mitchison, 1989) as well as the need to combine measurements from live and lysed cells. Using the photoactivation approach, we have confirmed a slow poleward movement of activated zones in mitotic mammalian cells. The temperature dependence of kMT turnover presented in Fig. 3 of this paper demonstrates why the slow poleward MT transport has only been observable in mammalian cells maintained at 30°C. Together with observations in newt lung cells (Mitchison and Salmon, 1992) and *Xenopus* extracts (Sawin and Mitchison, 1991, 1994; Sawin et al., 1992), the results suggest that poleward MT movement may be a widespread phenomenon in cells.

While our observations on poleward transport of MTs are in general agreement with the observations in newt lung cells (Mitchison and Salmon, 1992), there are some differences. In the newt cells, poleward transport of MTs was 0.54 μm/min in metaphase spindles, 0.44 μm/min in

early anaphase spindles, and 0.18 μm/min in late anaphase. These numbers could be interpreted as showing a more gradual and less abrupt change at the metaphase–anaphase transition than we have observed. 20 min after the onset of anaphase the newt spindle is still intact and the individual fully condensed chromosomes are still observed. At the same time point in the cells we studied, the cells have entered telophase with decondensing chromosomes and cell cleavage has commenced. Clearly the shift back to the interphase conditions occurs more slowly in the newt cells and this may allow the transition from the metaphase rate to the anaphase rate of MT transport to be detected in the first minutes of anaphase. Even so, the movement of the fluorescent mark in the anaphase plots shown is no more bi-phasic than it is in the metaphase plot (Mitchison and Salmon, 1992, Figs. 3 and 7). Both our study and the newt cell study showed a large variation in the rates of poleward MT transport from cell to cell, making sample size very important. The MT transport rate of a few anaphase cells can be faster than the rate in the slower metaphase cells. This makes our measurements of both metaphase and anaphase transport within the same cell very important and significant. Whenever the rates were measured within the same cell the metaphase rate was more than twice as fast as the anaphase rate.

The observations of poleward transport of MTs raise questions about kMT dynamics, spindle structure and the biological function of the movement. Since at least some kMTs have been shown to extend continuously between the kinetochore and the pole, the observations of MT transport indicate that kMTs are polymerizing continuously at their plus ends while maintaining attachment to kinetochores and depolymerizing at their minus ends while remaining focused at the pole. This dynamic behavior for both plus and minus ends of kMTs is similar to the concept originally termed MT treadmilling (Margolis and Wilson, 1981) which describes an intrinsic property of MTs where balanced polymerization and depolymerization occur at opposite ends of an MT, driven by differences in subunit affinities and the energy of ATP hydrolysis. However, the situation in living cells is likely to be more complex since MT plus ends are associated with the kinetochore and MT minus ends with the pole; both structures may affect MT dynamics.

The major focus of the experiments presented here is the quantitative analysis of kMT dynamics at the metaphase–anaphase transition and it reveals that the poleward MT movement is significantly reduced after anaphase onset. Although the function of the poleward MT transport is uncertain, it is nevertheless worthwhile to consider the possible significance of its slowing in anaphase. One possible explanation for the reduced rate of MT transport in anaphase may be a change in the intrinsic dynamic behavior of MT minus ends. Since anaphase onset marks the beginning of a return of many cellular processes to the interphase state (Murray and Hunt, 1993), it seems reasonable to assume that the dynamic behavior of kMTs at both ends might change from metaphase to anaphase. Studies using mitotic Xenopus egg extracts have demonstrated poleward MT flux in monopolar half spindles and even in artificially induced astral MT arrays lacking chromosomes and conventional centrosomes (Sawin and Mitchison, 1994). These authors conclude that poleward MT flux is an intrinsic property of MT arrays in mitosis, possibly involving molecular motors. If motor molecules are driving poleward transport, it is likely that they are bound near the minus ends of the MTs and are connected either directly or indirectly to the pole, allowing or causing depolymerization to occur. Inactivation of the motor protein at anaphase onset would slow poleward MT movement. These considerations suggest that minus end subunit dynamics and/or motor activity at the centrosome are subject to modulation at this key cell cycle point. Possibly, the reduced poleward MT transport seen in anaphase is a result of down regulation of a mitotic activity as the cell returns to interphase. Consistent with this viewpoint, MT transport toward the centrosome has not been seen in interphase MT arrays in two cell types (this report and Rodionov et al., 1994). This observation coupled with the results of Sawin and Mitchison, 1994, highlight a fundamental difference in the activity of mitotic and interphase centrosomal MT arrays.

The significance of MT poleward transport needs to be considered in the context of overall chromosome movement. Chromosomes move toward the poles by two mechanisms—one coupled to depolymerization of MTs at the kinetochore causing the chromosome to move relative to its attached MTs and a second coupled to depolymerization at the poles causing the MTs to move together with their attached chromosomes. These two processes contribute in different degrees over the course of anaphase. In early anaphase, chromosomes in LLC-PK cells moved toward the pole at an average rate of 1.15 ± 0.15 μm/min, whereas the average rate of poleward movement of marked zones was 0.19 μm/min. Thus, the relative contribution of poleward MT transport to chromosome movement during this phase was only 16%. This relatively small contribution to the anaphase chromosome movement suggests that poleward MT transport may not be essential for achieving chromosome segregation in anaphase. However, in late anaphase (beyond five minutes) chromosomes move much more slowly, progressing poleward at an average rate approximating that of MT transport, suggesting that the slow late chromosome movements may be driven by the slow poleward MT transport. Possibly, MT poleward transport serves as a redundant mechanism for chromosome segregation, functioning in the event the primary mechanism is deficient.

In conclusion, we have found that kMTs in metaphase turn over more slowly than previously thought and that comparison of metaphase and anaphase spindle dynamics demonstrates that kMT turnover is reduced during anaphase. These properties may be interpreted in terms of a MT capture and release cycle. We confirmed that the kinetochore is the primary site of tubulin loss in anaphase and that the pole is a secondary site. A distinct change in the rate of MT transport at the metaphase–anaphase transition indicates that MT dynamics at the pole is subject to cell cycle regulation.

We thank Drs. Gary J. Gorbsky, Gordon E. Hering and Peter W. Baas for their critical reading of this manuscript and helpful discussions. We are also grateful to Dr. Tim J. Mitchison for his gift of caged-fluorescein probe. We would like also to thank John Peloquin for preparation of caged-fluorescein tubulin and valuable discussions throughout this study.

This work was supported by National Institutes of Health grant GM 25062 to G. G. Borisy.

Received for publication 18 May 1995 and in revised form 5 July 1995.

References

Brinkley, B. R., and J. Cartwright. 1971. Ultrastructural analysis of mitotic spindle elongation in mammalian cells in vitro. *J. Cell Biol.* 50:416–431.

Brinkley, B. R., and J. Cartwright. 1975. Cold-labile and cold-stable microtubules in the mitotic spindle of mammalian cells. *Ann. N. Y. Acad. Sci.* 253: 428–439.

Cassimeris, L., S. Inoue, and E. D. Salmon. 1988. Microtubule dynamics in the chromosomal spindle fiber: analysis by fluorescence and high-resolution polarization microscopy. *Cell Motil. & Cytoskeleton.* 10:185–196.

Cassimeris, L., C. L. Rieder, G. Rupp, and E. D. Salmon. 1990. Stability of microtubule attachment to metaphase kinetochores in PtK_1 cells. *J. Cell. Sci.* 96:9–15.

Czaban, B. B., A. Forer, and A. S. Bajer. 1993. Ultraviolet microbeam irradiation of chromosomal spindle fibers in *Haemanthus katherinae* endosperm. *J. Cell Sci.* 105:571–578.

Gelfand, V. I., and A. D. Bershadsky. 1991. Microtubule dynamics: mechanism, regulation, and function. *Ann. Rev. Cell Biol.* 7:93–116.

Gorbsky, G. J., and G. G. Borisy. 1989. Microtubules of the kinetochore fiber turn over in metaphase but not in anaphase. *J. Cell Biol.* 109:653–664.

Gorbsky, G. J., P. J.Sammak, and G. G. Borisy. 1987. Chromosomes move poleward in anaphase along stationary microtubules that coordinately disassemble from their kinetochore ends. *J. Cell Biol.* 104:9–18.

Gorbsky, G. J., P. J. Sammak, and G. G. Borisy. 1988. Microtubule dynamics and chromosome motion visualized in living anaphase cells. *J. Cell Biol.* 106: 1185–1192.

Gorbsky, G. J., C. Simerly, G. Schatten, and G. G. Borisy. 1990. Microtubules in the metaphase-arrested mouse oocyte turnover rapidly. *Proc. Natl. Acad. Sci. USA.* 87:6049–6053.

Hamaguchi, Y., M. Toriyama, H. Sakai, and Y. Hiramoto. 1987. Redistribution of fluorescently labeled tubulin in the mitotic apparatus of sand dollar eggs and the effects of taxol. *Cell Struct. Funct.* 12:43–52.

Huitorel, P., and M. W. Kirschner. 1988. The polarity and stability of microtubule capture by the kinetochore. *J. Cell Biol.* 106:151–159.

Hush, J. M., P. Wadsworth, D. A. Callaham, and P. K. Hepler. 1994. Quantification of microtubule dynamics in living plant cells using fluorescence redistribution after photobleaching. *J. Cell Sci.* 107(4):775–784.

Kreis, T., and W. Birchmeier. 1982. Microinjection of fluorescently labeled proteins into living cells with emphasis on cytoskeletal proteins. *Int. Rev. Cytol.* 75:209–227.

Margolis, R. L., and L. Wilson. 1981. Microtubule treadmills: possible molecular machinery. *Nature (Lond.).* 293:705–711.

McDonald, K. L., E. T. O'Toole, D. N. Mastronarde, and J. R. McIntosh. 1992. Kinetochore microtubules in PtK cells. *J. Cell Biol.* 118:369–383.

McIntosh, J. R., and G. E. Hering. 1991. Spindle fiber action and chromosome movement. *Ann. Rev. Cell Biol.* 7:403–426.

McIntosh, J. R., W. Z. Cande, and J. A. Snyder. 1975. Structure and physiology of the mammalian mitotic spindle. *In* Molecules and Cell Movement. S. Inoue, and R. E. Stephens, editors. Raven Press, New York. 31–76.

Mitchison,T. J. 1988. Microtubule dynamics and kinetochore function in mitosis. *Ann. Rev. Cell Biol.* 4:527–549.

Mitchison, T. J. 1989. Polewards microtubule flux in the mitotic spindle: evidence from photoactivation of fluorescence. *J. Cell Biol.* 109:637–652.

Mitchison, T. J., and M. W. Kirschner. 1984. Dynamic instability of microtubule growth. *Nature (Lond.).* 312: 237–247.

Mitchison, T. J., and M. W. Kirschner. 1985*a*. Properties of the kinetochore in vitro. I. Microtubule nucleation and tubulin binding. *J. Cell Biol.* 101:755–765.

Mitchison, T. J., and M. W. Kirschner. 1985*b*. Properties of the kinetochore in vitro. II. Microtubule capture and ATP-dependent translocation. *J. Cell Biol.* 101:766–777.

Mitchison, T. J., and E. D. Salmon. 1992. Poleward kinetochore fiber movement occurs during both metaphase and anaphase A in newt lung cell mitosis. *J. Cell Biol.* 119:569–582.

Mitchison, T. J., L. Evans, E. Schulze, and M. W. Kirschner. 1986. Sites of microtubule assembly and disassembly in the mitotic spindle. *Cell.* 45:515–527.

Murray, A. W., and T. Hunt. 1993. The Cell Cycle: An Introduction. W. H. Freeman and Company, New York. 1–88.

Nicklas, R. B., and D. F. Kubai. 1985. Microtubules, chromosome movement, and reorientation after chromosomes are detached from the spindle by micromanipulation. *Chromosoma.* 92:313–324.

Nicklas, R. B. 1988. The forces that move chromosomes in mitosis. *Ann. Rev. Biophys. Biophys. Chem.* 17:431–449.

Pepperkok, R., M. H. Bre, J. Davoust, and T. E. Kreis. 1990. Microtubules are stabilized in confluent epithelial cells but not in fibroblasts. *J. Cell Biol.* 111: 3003–3012.

Rieder, C. L. 1981*a*. The structure of the cold-stable kinetochore fiber in metaphase PtK_1 cells. *Chromosoma.* 84:145–158.

Rieder, C. L. 1981*b*. Effect of hypothermia (20–25°C) on mitosis in PtK_1 cells. *Cell Biol. Int. Rep.* 5:563–573.

Rieder, C. L. 1982. The formation, structure, and composition of the mammalian kinetochore and kinetochore fiber. *Int. Rev. Cytol.* 79:1–58.

Rodionov, V. I., S. S. Lim, V. I. Gelfand, and G. G. Borisy. 1994. Microtubule dynamics in fish melanophores. *J. Cell Biol.* 126:1455–1464.

Salmon, E. D., D. Goode, T. K. Maugel, and D. B. Bonar. 1976. Pressure-induced depolymerization of spindle microtubules. III. Differential stability in HeLa cells. *J. Cell Biol.* 69:443–454.

Salmon, E. D., M. McKeel, and T. Hays. 1984*a*. Rapid rate of tubulin dissociation from microtubules in the mitotic spindle in vivo measured by blocking polymerization with colchicine. *J. Cell Biol.* 99:1066–1075.

Salmon, E. D., R. J. Leslie, W. M. Saxton, M. L. Karow, and J. R. McIntosh. 1984*b*. Spindle microtubule dynamics in sea urchin embryos. *J.Cell Biol.* 99: 2164–2174.

Sammak, P. J., G. J. Gorbsky, and G. G. Borisy. 1987. Microtubule dynamics in vivo: a test of mechanisms of turnover. *J. Cell Biol.* 104:395–405.

Sawin, K. E., and T. J. Mitchison. 1991. Poleward microtubule movement in mitotic spindles assembled in vitro. *J. Cell Biol.* 112:941–954.

Sawin, K. E., and T. J. Mitchison. 1994. Microtubule flux in mitosis is independent of chromosomes, centrosomes, and antiparallel microtubules. *Mol. Biol. Cell.* 5:217–226.

Sawin, K. E., K. LeGuellec, M. Philippe, and T. J. Mitchison. 1992. Mitotic spindle organization by a plus-end-directed microtubule motor. *Nature (Lond.).* 359:540–543.

Saxton, W. M., D. L. Stemple, R. J. Leslie, E. D. Salmon, M. Zavortink, and J. R. McIntosh. 1984. Tubulin, dynamics in cultured mammalian cells. *J. Cell Biol.* 99:2175–2186.

Skibbens, R. V., P. S. Victoria, and E. D. Salmon. 1993. Directional instability of kinetochore motility during chromosome congression and segregation in mitotic Newt lung cells: a push-pull mechanism. *J. Cell Biol.* 122:859–875.

Spurck, T. P., O. G. Stonington, J. A. Snyder, J. D. Pickett-Heaps, A. Bajer, and J. Mole-Bajer. 1990. UV microbeam irradiations of the mitotic spindle fiber dynamics and force production. *J. Cell Biol.* 111:1505–1518.

Wadsworth, P., and E. D. Salmon. 1986. Analysis of the treadmilling model during metaphase of mitosis using fluorescence redistribution after photobleaching. *J. Cell Biol.* 102:1032–1038.

Wadsworth, P., E. Shelden, G. Rupp, and C. L. Rieder. 1989. Biotin-tubulin incorporation into kinetochore fiber microtubules during early but not late anaphase. *J. Cell Biol.* 109:2257–2265.

Wojcieszyn, J. W., R. A. Schlegel, E.-S.Wu, and K. A. Jacobson. 1981. Diffusion of injected macromolecules within the cytoplasm of living cells. *Proc. Natl. Acad. Sci. USA.* 78:4407–4410.

Wise, D., L. Cassimeris, C. L. Rieder, P. Wadsworth, and E. D. Salmon. 1991. Chromosome fiber dynamics and congression oscillations in metaphase PtK_2 cells at 23°C. *Cell Motil. & Cytoskeleton.* 18:131–142.

Zhai, Y., and G. G. Borisy. 1994. Quantitative determination of the proportion of microtubule polymer during the mitosis-interphase transition. *J. Cell Sci.* 107(4):881–890.